Aging and degradation of aluminum-silicon structures with a Schottky barrier after a pulsed laser irradiation

_G.I.Vorobets, O.I.Vorobets, A.P.Fedorenko, A.G.Shkavro_*

Physics Department, Yu.Fed'kovych Chernivtsi National University,
2 Kotsyubinsky St., 58012 Chernivtsi, Ukraine
*Radiophysics Department, T.Shevchenko Kyiv National University,
64 Volodymyrska St., 01017 Kyiv, Ukraine

Influence of a SiO_2 layer on the contact perimeter and of laser pre-irradiation regime on degradation of electrophysical characteristics and parameters of case-free thin-film Al–*n*–Si structures with a Schottky barrier has been studied in experiment. It is shown that at the irradiation intensity $I_0 < 100$ kW/cm^2, a more prolonged stability of the potential barrier height φ_b and ideality coefficient n for the irradiated Schottky diodes formed on the silicon free surface as compared to non-irradiated structures and those formed in the SiO_2 windows.

Экспериментально исследовано влияние слоя SiO_2 по периметру контакта и режимов предварительного лазерного облучения на деградацию электрофизических характеристик и параметров бескорпусных тонкопленочных структур Al–*n*–Si с барьером Шоттки. Показано, что при интенсивности облучения $I_0 < 100$ кВт/см^2 обеспечивается более длительная стабильность высоты потенциального барьера φ_b и коэффициента идеальности n облученных диодов Шоттки, сформированных на свободной поверхности кремния, по сравнению с необлученными и структурами, сформированными в окнах SiO_2.

The problem of stability of electrical parameters and characteristics of the metal-semiconductor contacts (MSC) and metal-insulator-semiconductor ones (MIS) at prolonged operation of semiconductor devices becomes especially actual when the microstructures are used in integrated electronics. To stabilize the parameters of ohmic contacts and MSC with a Schottky barrier, various technologies are used. To study the causes and mechanisms of degradation, accelerated tests of devices under elevated temperatures and electrical voltages are used [1, 2]. In this work, the study results of the (I–V) and (C–V) characteristics degradation are presented for Al–*n*–Si structures with a Schottky barrier under natural conditions, i.e. the operation in a rated mode and storage of the devices at room temperatures during fifteen years after the manufacturing and photon correction of their parameters.

Two types of the Al–*n*–n^+–Si–Al structures were used. The first group of structures was prepared using the standard technique. The (111) plates of KEF-1 grade silicon with surface resistance of 1 Ω·cm were chemically treated. Then, the previously formed SiO_2 layer was removed from the non-working surface of the plate for their doping with phosphorus. The SiO_2 layer was chemically removed from the whole effective area of a plate followed by its purification by ion jet etching. Then, aluminum film was deposited on the effective area, and its photolitography was performed followed by aluminum deposition onto the opposite plate surface and its burning-in. The heat treatment of the obtained Al–*n*–n^+–Si–Al structures results in a rectifying contact on the effective *n*–Si area and an ohmic

Table

I_0, kW/cm^2	I group of Al–n–n^+–Si–Al SD						II group of Al–n–n^+–Si–Al SD					
	φ_b, eV		α, V^{-1}		n		φ_b, eV		$\alpha Б$ AaB, V^{-1}		n	
	P	*D*	*P*	*D*	*P*	*D*	*P*	*D*	*P*	*D*	*P*	*D*
0	0.73	0.72	36.3	35.3	1.08	1.13	0.70	0.71	33.9	35.7	1.17	1.12
85	0.76	0.72	36.8	37.2	1.06	1.09	0.75	0.72	36.1	37.3	1.08	1.07
96	0.78	0.72	39.0	36.3	1.01	1.11	0.76	0.71	36.8	35.2	1.06	1.14
106	0.80	0.75	38.6	37.3	1.05	1.08	0.75	0.71	35.4	35.8	1.11	1.12
117	0.75	0.67	33.4	27.6	1.18	1.46	0.75	0.72	36.2	35.5	1.11	1.13

contact on the Si surface doped with phosphorus. In this case, an epitaxial p^+-layer can be deposited on the Si surface at the Al–n–Si interface at the thermal annealing [2, 3]. The second group of structures were prepared similarly to the first one except for the diodes with a Schottky barrier (SD) were obtained by ion-beam aluminum deposition in SiO_2 windows on the effective area of silicon plate.

The main physical parameters which defining the metal-semiconductor contacts electrophysical properties are the potential barrier height, φ_b, differential linearity coefficient of the current-voltage characteristic in semilogarithmic scale, α, and the current-voltage characteristic ideality coefficient, n [2].

The parameters of the initial Al–Si contacts depend on the manufacturing method. The potential barrier height for contacts of the first group is $\varphi_b = 0.73 \pm 0.01$ eV while for the second one, $\varphi_b = 0.70 \pm 0.01$ eV. The corresponding coefficients had values of $n = 1.076$, $\alpha = 36.31$ V^{-1} and $n = 1.173$, $\alpha = 33.92$ V^{-1}, respectively. Thus, the structures under investigation are close to ideal ($n \sim 1$) and their parameters agree well with data obtained by other authors. So, the values $\varphi_b = 0.72 \pm 0.01$ eV and $n = 1.02$ have been reported [4] for Al–n–Si (111) structures heat-treated at $T = 460$°C for 10 min in nitrogen atmosphere. The φ_b values ranging from 0.51 eV to 0.68 eV are reported for unannealed Al–n–Si contacts prepared by standard technology. Such a difference in φ_b values is explained by variation of natural oxide parameters on the silicon surface due to chemical etching of the Si plate and its subsequent exposure to air prior to the ion-beam aluminum deposition. Therefore, the initial structures can be described using physical models of Al–Si contacts with thin p^+-layer at the Al–n–Si interface and tight Al–n–Si contacts.

However, in structures with a Schottky barrier on silicon having the current-voltage characteristics at room temperature close to ideal ones but $n \approx 1.08 \div 1.17$, additional charge transfer mechanisms can manifest themselves at lower temperatures [5]. To reduce the additional charge transfer, the photon correction of parameters of the structures under study was used.

An YAG laser operated in the free oscillation mode with 1.06 μm wavelength was used as a pulsed photon radiation source. The radiation intensity I_0 was varied from 20 MW/cm^2 to 10 kW/cm^2 by the beam defocusing from 200 μm to 2 mm. Thus, the solid phase processes are realized at the metal-semiconductor interface but no micro- and nanosecond modes of pulse treatment resulting in a deep recrystallization of the surface layers and destruction of the irradiated material take place.

The irradiation of the structures at the radiation intensity I_0 of 80 to 130 kW/cm^2 results in some transformation of the current-voltage characteristics and initial physical properties of SD. The Table presents comparative analysis of φ_b, α, n parameters determined from the direct current-voltage characteristics for initial structures ($I_0 = 0$) and structures after photon correction ($I_0 \neq 0$) for the first (I) and the second (II) group of SD examined prior to (P) and after (D) the degradation. At room temperature, the direct current-voltage characteristic of the initial SD both the first (Fig. 1) and the second (Fig. 2) group can be approximated by a linear dependence of the current logarithm on voltage. As the radiation intensity I_0 increases up to the critical value I_c the direct current cutoff values I_s decrease by 5 to 10 times. The potential barrier becomes 0.03 to 0.07 eV

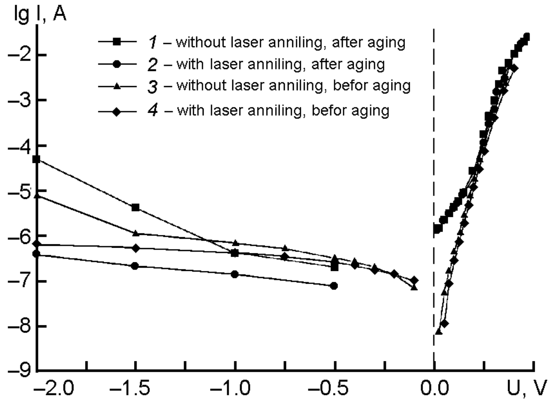

Fig. 1. Current-voltage characteristics of Al–n–n^+–Si–Al structures formed on SiO_2-free silicon surface.

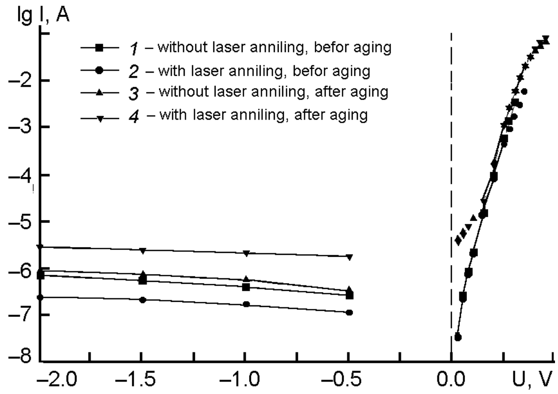

Fig. 2. Current-voltage characteristics of Al–n–n^+–Si–Al structures formed in the SiO_2 windows on silicon surface.

higher and attains its maximum at I_c. The further radiation intensity increase ($I_0 > I_c$) results in deterioration of the SD parameters and current-voltage characteristic transformation from rectifying to ohmic one for both groups of contacts. The difference consists in that for the first group of structures $I_c \sim 105$ kW/cm^2, while for second one, $I_c \sim 95$ kW/cm^2. The current-voltage characteristics become ohmic at $I_0 \sim 150$ kW/cm^2 and $I_0 \sim 130$ kW/cm^2, respectively. At $I_0 < I_c$, the ideality coefficient for those contacts drops almost linearly from $n = 1.08$ to $n = 1.01$ and from $n = 1.17$ to $n = 1.06$ for the first and the second group of structure, respectively, when I_0 increases.

The reverse currents of SD formed in SiO_2 windows go to saturation and do not exceed 10 μA at reverse bias voltage $U_r > 10$ V. In experiment, for the first group of contacts, the saturation of reverse currents is observed at $U_r < 1.5$ V and their sharp increase by 1.5 to 2 orders occurs at $U_r > 1.5$ V. The irradiation of those structures in an optimum mode causes the reverse current decrease by one order and at $I_0 > I_c$, its increase by two orders. The saturation voltage of the current-voltage characteristic reverse branches for the first SD group shows an increase up to 2.5–3.0 V.

During the natural aging of the structures, a knee on a direct current-voltage characteristic constructed in semilogarithmic scale appears at the bias $U_d \sim 0.25$ V for SD on the free Si surface (Fig. 1) and $U_d \sim 0.15$ V for SD in SiO_2 windows. The reverse currents for the first group contacts irradiated at intensities $I_0 \le I_c$ decrease a little, whereas for unirradiated contacts at $U_r < 1$ V, those currents increase by 1 to 1.5 orders. For the second group SD (Fig. 2), the reverse current increase for irradiated structures is 5 times higher as compared to that for unirradiated ones. At the irradiation by $I_0 \approx I_c$ and higher, the reverse currents increase faster and amount to about a milliampere at the reverse bias 1.5 V and 7 V for the first and second groups of contacts, respectively.

The observed current-voltage characteristic changes are connected with the contribution of additional charge transfer mechanisms in the structures under study to the over-barrier one, accompanied by the degradation of structural parameters due to aging (Tabl.). It is to note that the potential barrier height for both groups of contacts after their aging, determined from the linear section the current-voltage characteristics at the direct voltages $U_d \ge 0.25$ V, approaches the value $\varphi_b = 0.72$ eV (n increasing up to 1.10±0.01 and 1.13±0.01 for the first and the second SD groups, respectively). However, for the first group of contacts irradiated at the optimum intensity and characterized by the initial value $\varphi_b = 0.80\pm0.01$ eV, the higher value $\varphi_b = 0.75\pm0.01$ eV observes. For structures irradiated at $I_0 > I_c$, φ_b drops down to $\varphi_b = 0.67$ eV.

The activation energy and ideality coefficients for the additional charge transfer, as determined from the slope of current-voltage characteristic initial sections ($U_d \le 0.25$ V), are $E_a = 0.62$ eV (n from 2.46 to 3.69); $E_a = 0.64$ eV ($n = 2.89\pm0.01$) for the first and the second DS group, respectively.

For Al–n–n^+–Si–Al DS, formed on SiO_2-free silicon surface and unirradiated or irradiated at low intensities I_0, the $1/C^2 = f(U)$

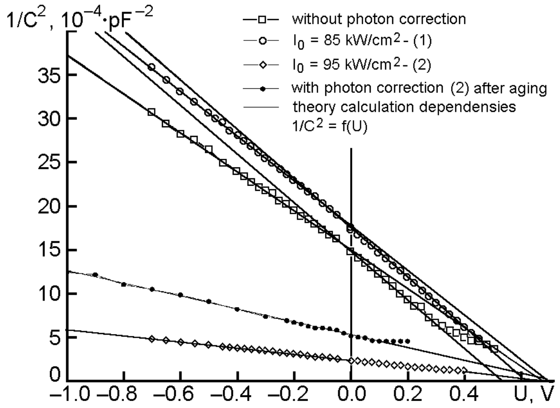

Fig. 3. Dependences $1/C^2 = f(U)$ for Al–n–n^+–Si–Al structures formed on SiO_2-free silicon surface.

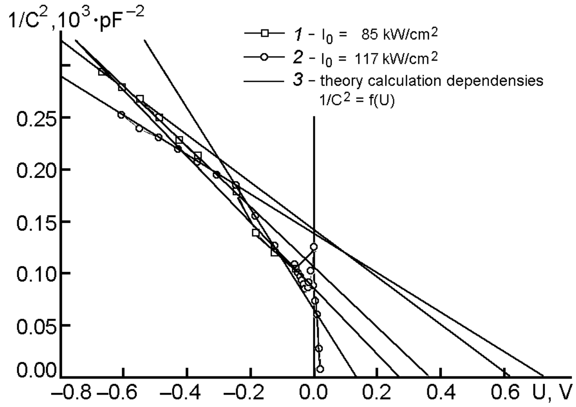

Fig. 4. Dependences $1/C^2 = f(U)$ for Al–n–n^+–Si–Al structures formed in the SiO_2 windows on silicon surface.

dependence can be described theoretically by two linear sections with an inflection point at zero bias (U = 0 V) (Fig. 3). At the optimum irradiation intensity I_0, the structure capacity increases, what is manifested as a considerable slope change of the investigated dependence. No inflection was observed while the linearity is maintained up to bias U_d = 0.4 V. As a result of the aging and degradation, the latter dependence starts to deflect from the linear law at the bias $U_d > 0.1$ V. The doping impurity concentration in initial chips is $n_b = 2 \cdot 10^{16}$ cm^{-3}, as determined from the $1/C^2 = f(U)$ dependence [6] at high reverse bias. The chemical potential for n-type silicon corresponding to the obtained value amounts $\mu = E_c - E_f$ = 0.19 eV. For this case, the bending value of energy bands φ_0 were found from linear approximations of the plots taken at positive biases (Fig. 4). This value at the interface of Al–n–Si for the photon-uncorrected structures and corrected ones at I_0 = 85 kW/cm^2 amounted 0.54 and 0.62 eV, respectively. These parameters are rather well consistent with the φ_b value for those SD calculated from the direct branches of current-voltage characteristics, since $\varphi_b = \mu + \varphi_0$ = 0.73±0.01 eV for unirradiated structures and φ_b = 0.81±0.01 eV for SD with photon-corrected paramete rs. Similar barrier determinations from linear approximations at reverse biases give somewhat overestimated values φ_b = 0.86±0.01 eV and φ_b = 0.88±0.01 eV for the named structures.

As a result of the structure parameters degradation due to aging, φ_0 increases up to 0.72±0.01 eV and φ_b, as found from (C–V) measurements, rises by 0.3 eV. Perhaps it is just such an increase in φ_b that explains also the reverse current decrease by a factor of 3 to 5 (Fig. 1) for the irradiated structures in comparison with unirradiated ones. Also, the φ_b increase by 0.3 eV in this case correlates with similar φ_b increase at thermal aging of the structures (Al + 0.14 g/mole Si)–n–Si at T = 200°C [2, p.173].

A specific feature of (C–V) characteristics for Al–n–n^+—Si–Al SD formed in SiO_2 windows due to the aging is the presence of several linear sections in the $1/C^2 = f(V)$ dependence at reverse biases $U_r \le 1$ V. This may evidence the change in impurity distribution profile in near-contact area of silicon [6]. The formation tunneled thin inverse conductivity transition layer at the Al–Si interface is quite probably [4]. This is consistent with the experimental study results of impurity redistribution in similar contacts at accelerated thermal aging processes [2]. The depth of impurity redistribution in subsurface layer is estimated to do not exceed about $0.2 \cdot 10^{-6}$ m. The impurity concentration in subsurface layer, as found from the $1/C^2 = f(U)$ dependence at $U_r < 1$ V, is (0.35 to 0.42)$\cdot 10^{16}$ cm^{-3}, whereas for the first group contacts at the optimum irradiation, it can rise up to (1.3 to 1.8)$\cdot 10^{17}$ cm^{-3}.

The peak value φ_0 = 0.73±0.01 eV obtained from the $1/C^2 = f(U)$ dependence at $U_r \ge 0.3$ V for Al–n–n^+–Si–Al SD in the SiO_2 windows after the photon correction of parameters and the aging of structures corresponds to the similar parameter for SD formed on the free Si surface. This fact confirms likely the similarity of the degradation processes in the studied structure types and is explained by diffusion redistribution of materials in contact and doping impurities near the metal-semiconductor interface. The cutoff voltages φ_k [6], as determined from the slope of the different linear sections of the $1/C^2 = f(U)$ dependences, amount (0.13±0.01), (0.27±0.01), (0.36±0.01) eV and are probably due to the presence of deep levels at the Al–n–Si interface. A more strong nonlinearity of the $1/C^2 = f(U)$ plots and the increase of reverse currents due to the aging for the second group contacts as compared to the first group ones can be explained by elastic stress relaxation in the aluminum film in the SiO_2 window.

Calculation of the transition p^+-layer parameters [2] for the first group structures evidences the possibility of its existence on MSC at optimum irradiation modes. In those cases, φ^* increases up to 0.85 eV, and the p^+-layer size is comparable to the shielding length in the semiconductor at $N_d = 10^{16}$ cm^{-3} and lequal to 0.13 μm. The φ_b increase at $I_0 = I_c$ is well explained by the p^+-layer formation and is in agreement with the data on the thermal annealing. However, at heat treatment, such process is accompanied by an increase of n up to 1.07 while at photon correction, n decreases down to 1.01.

Investigation of reverse current-voltage characteristic of the irradiated (at I_0 = 85 kW/cm^2) and unirradiated structures of the first group at small biases shows that those can be described by the dependence $I_r \sim (U_r)^\beta$ with $\beta = 0.50$, typical of generation current. As I_0 increases up to I_c, β decreases down to 0.20. Moreover, for some contacts, the dependences typical of generation charge transfer mechanism may be retained at the initial section of current-voltage characteristic ($0 < U_r < 0.4$ V) even at $I_0 = I_c$.

The reverse current-voltage characteristics of the second group Al–n–Si contacts are well described also by the dependence for generation mechanism charge transfer $I_r \sim (U_r)^{1/2}$ at $I_0 \le I_c$. Here, in contrast to the first group contacts, the increase of I_0 up to I_c does not result in any considerable decrease of the generation-recombination current. In this case, different mechanisms of charge transfer predominate in direct and reverse direction.

The data for reverse current-voltage characteristics are consistent with calculations of the transition layer parameters according to a direct ones. In this case, the potential barrier height increases by 0.04 or 0.05 eV and coefficient n approaches unity when radiation intensity increases. This can be explained by the expression of image forces [4] in nearly-ideal Al–n–Si contacts. In this case ($I_0 < I_c$), the pulse laser radiation effect on MSC results in a heating of the system and appearance of heat-induced elastic stresses in contacting metal and semiconductor layers due to the difference in their thermal expansion coefficients. The relaxation of those elastic tensions at the contact cooling causes an ordering of atomic structure in sub-surface silicon layer (in the space charge area (SCA) of DS) and annealing of the centers creating additional deep levels for generation-recombination charge transfer. In contacts formed in the SiO_2 windows, additional mechanical stresses arise under pulse heating at the Al–SiO_2 interface along the contact perimeter. This results in relaxation of heat-induced elastic stresses at the Al–n–Si interface at low irradiation intensities or in destruction of the aluminum contact at large radiation intensities used to photon correction. Therefore, deep levels in these structures are annealed to a lesser extent.

The time relaxation of elastic stresses in the aluminum film activates processes of Si dissolution in Al and thus an increased defect concentration at the Al–n–Si interface. The concentration of levels at the Al–n–Si interface increases, which, in turn, results in a more intense development of additional charge transfer mechanisms in the structures under consideration. However, it is impossible to explain the degradation of the current-voltage characteristic in semilogarithmic scale only by generation-recombination of carriers in SCA of the semiconductor (when $n = 2$). Perhaps the structure inhomogeneity over its area, edge currents, or other charge transfer mechanisms may be involved here.

Thus, the laser treatment of Al–n–Si structures with a Schottky barrier at optimum modes, when interaction at the aluminum-silicon interface occurs in solid phase ($T < 650°$C), causes an increase of the potential barrier height and approximation of the ideality coefficient of the structure to unity. The possible mechanism of photon correction of the parameters consists in a decrease of the deep levels concentration in silicon sub-surface layer and the relaxation of heat-induced elastic stresses. This favors in part the more prolonged constancy of parameters of the Al–*n*–Si structures formed on the oxide-free silicon surface and irradiated at optimum intensities, as compared to unirradiated structures and those formed in the SiO_2 windows. However, aging and degradation processes in the Al–*n*–Si structures run in the same manner independently of their pre-processing and manifest themselves as a deviation of current-voltage characteristics in semilogarithmic scale from the linearity at small direct biases, increased reverse currents, and changes in the active center profile in SCA of the metal-semiconductor contacts. A prolonged storage and operation of the aluminum-silicon structures in nominal modes at room temperature results in stabilization of the potential barrier value at a level of $\varphi_b = 0.72$ eV ($n = 1.1$), which is characteristic for the Al–*n*–Si tight contacts.

References

1. G.V.Gadiyak, J.Stathis, *Fiz. Tekhn. Poluprov.*, **32**, 1079 (1998).
2. V.I.Strikha, E.V.Buzaneva, Physical Principles of Metal-Semiconductor Contacts in Integrated Electronics, Radio i Svyaz‘, Moscow (1987) [in Russian].
3. E.V.Buzaneva, G.I.Vorobets, V.I.Strikha et al., in: Abstr. of Int. School-Conf. on Physical Problems in Material Science of Semiconductors, Chernivtsi, Ukraine (1995), p.305 [in Russian].
4. Thin Films: Interdiffusion and Reactions, ed. by J.M.Poate, K.N.Tu, J.W. Mayer, Wiley, New-York (1978).
5. E.V.Buzaneva, G.I.Vorobets, V.I.Strikha et al., in: Electronic Engineering, Ser. 2: Semiconductor Devices, 3rd (200^{th}) Issue (1989), p.49 [in Russian].
6. V.G.Georgiu, Voltage-Capacity Measurements of Semiconductor Parameters, Stiinta, Kishinev (1987) [in Russian].

Старіння та деградація структур алюміній-кремній з бар’єром Шотткі після імпульсного лазерного опромінення

Г.І.Воробець, О.І.Воробець, А.П.Федоренко, А.Г.Шкавро

Експериментально досліджено вплив шару SiO_2 за периметром контакту і режимів попереднього лазерного опромінення на деградацію електрофізичних характеристик і параметрів безкорпусних тонкоплівкових структур Al–*n*–Si з бар’єром Шотткі. Показано, що при інтенсивності опромінення $I_0 < 100$ кВт/см^2 забезпечується більш тривала стабільність висоти потенційного бар’єра φ_b і коефіцієнта ідеальності n опромінених діодів Шотткі, сформованих на вільній поверхні кремнію, в порівнянні з неопроміненими і структурами, сформованими у вікнах SiO_2.